INSTITUTE OF PHYSICS PUBLISHING PLASMA SOURCES SCIENCE AND TECHNOLOGY

Plasma Sources Sci. Technol. **11** (2002) 476–483 PII: S0963-0252(02)53661-6

Characterization of a high-pressure microdischarge using diode laser atomic absorption spectroscopy

C Penache[1], M Miclea[2,4], A Bräuning-Demian[3], O Hohn[1], S Schössler[1], T Jahnke[1], K Niemax[2] and H Schmidt-Böcking[1]

[1] J W Goethe University, Institut für Kernphysik (IKF), August-Euler-Str. 6, D-60486 Frankfurt am Main, Germany

[2] Institute for Spectrochemistry and Applied Spectroscopy (ISAS), Bunsen-Kirchhoff-Str. 11, D-44139 Dortmund, Germany

[3] Gesellschaft für Schwerionenforschung (GSI), Planckstr. 1, D-64291 Darmstadt, Germany

E-mail: miclea@isas-dortmund.de

Received 26 February 2002, in final form 12 September 2002
Published 17 October 2002
Online at stacks.iop.org/PSST/11/476

Abstract

A high-pressure dc glow discharge based on micro-structured-electrode (MSE) arrays was investigated by diode laser atomic absorption spectroscopy. The microdischarge was studied at constant current in pure Ar for pressures ranging from 50 to 400 mbar. The measurements of the absolute population density of the excited $1s_5$, $1s_4$, $1s_3$, and $1s_2$ levels of Ar in the discharge revealed a population density of excited atoms in metastable and resonance states in the range 10^{12}–10^{15} cm^{-3}. The gas temperature and the electron number density were evaluated from the analysis of the absorption line profiles, taking into account significant broadening mechanisms. The gas temperature, derived from the Doppler broadening, was found to increase with pressure from 380 K at 50 mbar to 1100 K at 400 mbar. The electron number density was calculated from the Stark broadening and shift, and it ranges from 9×10^{14} to 5×10^{15} cm^{-3}. The MSE-sustained discharges are combining the non-equilibrium character with the advantage of high-pressure, which recommends them for non-thermal plasma processing e.g. surface treatment, plasma chemistry and generation of UV and VUV radiation.

1. Introduction

Plasma sources operating close to atmospheric pressure are very useful tools for atomic emission spectrometry, surface treatment, reduction of pollutants, and generation of UV and VUV radiation. High-pressure plasmas have been intensively studied in recent years in various configurations using different types of excitation from direct current or low frequency alternative current to radio frequency or microwave. The increased interest in dc and pulsed corona discharges [1], dielectric barrier discharges [2, 3], micro hollow cathode discharges [4, 5], radio frequency [6] and microwave discharges [7] is due to the fact that for applications on an industrial scale it is very important to achieve reliable high-pressure operation employing moderate voltages. Using micro-structured-electrode (MSE) arrays with a discharge gap of hundreds of μm atmospheric pressure plasma can be generated at forward voltages of few hundreds of volts. Based on MSE, stable homogeneous dc glow discharges can be operated in air, noble gases and mixtures containing reactive gases at pressures ranging from 50 to 1000 mbar [8, 9]. Intrinsic parameters of this new plasma source are up to now not well known. This is due to the limitations in choosing appropriate diagnostic methods, determined by the small dimensions of the discharge (hundreds of μm).

This work is concerned with the study of the population density of the excited atoms produced in an MSE-sustained

[4] Author to whom correspondence should be addressed.

discharge operated in argon and with the evaluation of the gas temperature and electron number density. The investigations are focused on the first four excited argon levels ($1s_i$, $i = 2$–5, Paschen notation). There is a strong motivation for measuring the excited atoms in this high-pressure discharge. Due to their long lifetime, atoms in metastable states are a deposit of energy in the discharge and they could play an important role in sustaining the ionization [10]. Particularly in high-pressure discharges, besides the electron impact ionization, the stepwise ionization becomes significant. The atoms in the lowest excited states are also the precursor in the generation of UV radiation. Studies concerning the generation of UV and VUV radiation in high-pressure discharges with dimensions in the submillimetric range [11, 12] are known. Microdischarges operated at high-pressure in rare gases and rare gas halides [13] could be an alternative to the currently available excimer lamps based on dielectric barrier discharges [14] if excessive heating of the gas is prevented. Furthermore, the excited neutrals can also release very efficient secondary electrons at the cathode, or may strongly interact with other surfaces and therefore are suitable for plasma assisted cleaning and/or activation.

The populations of the excited Ar atoms on resonance and metastable levels were studied using diode laser (DL) atomic absorption spectroscopy (DLAAS). DLs are very useful tools for spectroscopic applications due to their special properties [15], such as very narrow line width (less than 100 MHz), single mode operation and continuous tuning over the absorption line profiles. Information about the integral number density of the excited states in the plasma channel was obtained by means of DLAAS. Due to the small dimensions of the discharge, accurate determination of the density of excited atoms is a challenging task.

The measurement of the electron number density and gas temperature in the microdischarge is based on the analysis of the absorption line profiles. A major advantage of the absorption spectroscopy technique using narrow spectral lasers is that the instrumental broadening is eliminated. The analysis of the line profiles of the Ar transitions at 801.699 nm ($1s_5$–$2p_8$) and 800.838 nm ($1s_4$–$2p_6$) revealed, besides Doppler broadening, also pressure broadening and shift due to the interaction of the absorbing atoms with neutral and charged particles (collision and Stark broadening). It is rather unusual to use the line profiles of non-hydrogenic atoms for evaluating the electron number density because these spectral lines undergo a quadratic Stark effect with much smaller impact on the line width than the linear Stark effect. In a recent paper [16], it was demonstrated that using DLAAS the electron number density could be measured if this is higher than 5×10^{14} cm^{-3}.

2. Characterization of the MSE discharge

The MSE array is a matrix of holes regularly distributed in a multilayer that consists of two metallic foils separated by an insulator. In each hole a microdischarge is ignited between the two metal layers representing the electrodes. The insulator (Kapton) has a thickness of 50 μm and sets the distance between the electrodes. For the present experiment single-hole structures with 130 μm thick copper electrodes have been used. The diameter of the holes was 300 μm.

The MSE-sustained discharge can be considered as a normal glow discharge whereby the excitation and ionization efficiency is increased by the specific discharge configuration (hollow cathode geometry). A single microdischarge in pure Ar was studied at pressure between 50 and 400 mbar and a constant gas flow of 100 ml min^{-1} through the chamber where the microstructure was mounted. The microdischarge was operated in the normal glow mode at relatively low current (0.5 mA) and a sustaining voltage of about 200 V. A detailed description of the discharge operation was reported in [17]. Due to the very small dimensions of the inner surface of the cathode the discharge expands out of the hole above the cathode for discharge currents higher than about 0.1 mA. Thus, the active surface of the cathode is enhanced, the secondary electron emission increases and the current is sustained at constant discharge voltage.

The optical appearance of the discharge was recorded side-on and end-on using a charge coupled device (CCD) camera (Princeton Instruments TE/CCD-1024). Because two of the transitions of interest for absorption measurements are at 801.699 and 800.838 nm, a narrow band filter centred at 800 nm and with a full-width at half-maximum (FWHM) of 10 nm was used to select this wavelength range from the total emitted light. The interference filter has a transmission of 95% and does not affect significantly the intensity of the emitted radiation. The side-on and end-on appearance of the microdischarge, recorded with an exposure time of 10 ms, is presented in figure 1 for different pressures. By increasing the pressure at constant current the emissive volume above the cathode surface decreases and the discharge concentrates inside the hole. Similar to a low-pressure glow discharge, as the pressure rises the negative glow and the cathode fall contract.

3. Experimental arrangement for DLAAS

For the investigation of the first four excited Ar levels shown in figure 2, three single-mode DLs were used as radiation sources. Their operational parameters are presented in table 1. A DL driver (Profile ITC 502) was used to supply the DL current and also to control and stabilize its temperature.

A classical absorption experiment schematically viewed in figure 3 was used to investigate the MSE sustained discharge. The collimated DL beam with a diameter of about 6 mm was passing through the discharge channel (300 μm diameter, 310 μm length) and was detected by a fast photodiode (PD) (Si PIN S6036) placed far enough from the plasma (0.5 m) in order to avoid the light emitted from the discharge reaching the detector. Due to the geometrical limitation only a small area of the laser beam was used in the case of the measurements performed through the hole of the microstructure. Before entering the discharge the radiation was attenuated by neutral filters (NF) in order to avoid the saturation of the optical transition. Due to the small dimensions of the MSE, diffraction patterns are observed on the detector when passing the laser beam through the hole inducing noise in the transmitted signal. Only the zero order of diffraction was selected from the total transmitted beam. By varying the DL current the wavelength was continuously scanned across the absorption line with very low frequency (7–8 mHz). The DL wavelength was measured with a wavemeter (Burleigh WA-10, spectral resolution 1 pm).

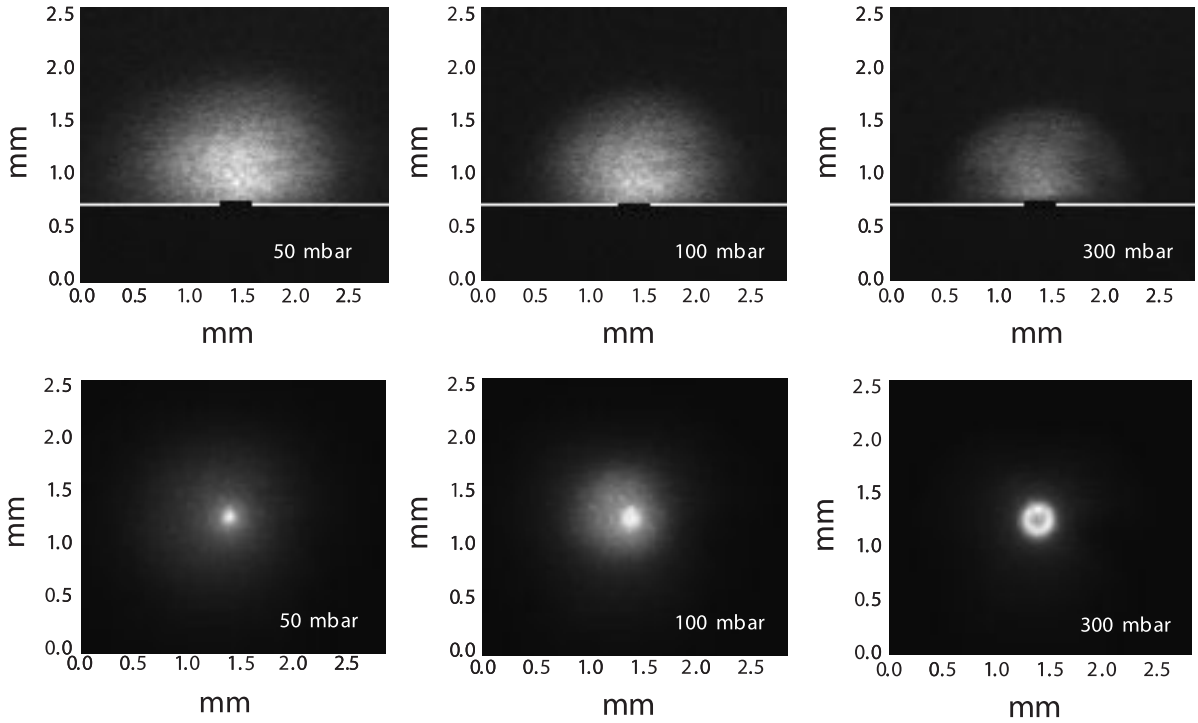

Figure 1. Optical appearance of the MSE-sustained discharge measured side-on and end-on at the cathode side. The position of the cathode surface and the MSE hole are shown.

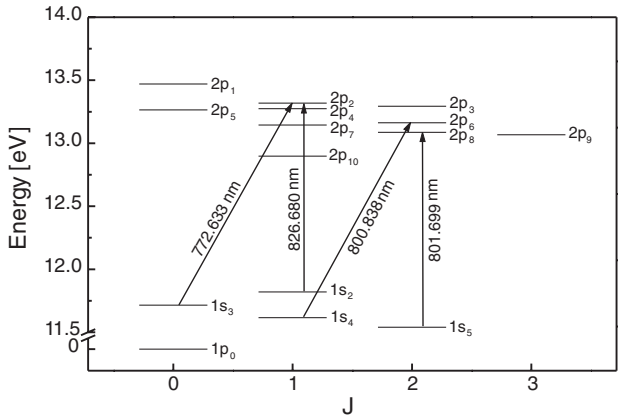

Figure 2. Partial energy level diagram of Ar and the transitions studied in this work.

Table 1. DLs used as radiation sources for DLAAS and the operation parameters corresponding to the central wavelength of each studied transition.

Central wavelength (nm)	Transition	DL operation parameters
801.699	$1s_5$–$2p_8$	Sharp/12.57°C, 67 mA
800.838	$1s_4$–$2p_6$	Sharp/−1.75°C, 70 mA
772.633	$1s_3$–$2p_2$	Sharp/12.51°C, 65 mA
826.680	$1s_2$–$2p_2$	Hitachi/2.5°C, 95 mA

Before reaching the microdischarge, a small part of the laser radiation was separated by a beam splitter (BS) and directed into a confocal Fabry–Perot interferometer (free spectral range FSR = 2 GHz). This provides the frequency calibration for the absorption line profiles. The signal transmitted from the PD and the interference fringes were simultaneously recorded on a two-channel oscilloscope (Tektronix TDS 360, 200 MHz, 1 GS s^{-1}).

When the direct absorption signal was low (absorption smaller than 2–5%), the discharge was modulated with low frequency (225 Hz) by a homemade current sink and the absorption signals were recorded using a lock-in amplifier (Stanford Research Systems SR830). The plasma modulation (PM) technique coupled with phase sensitive detection is a very well-known method in analytical atomic spectroscopy [18] where small optical depths (10^{-2}–10^{-4}) have to be measured.

4. Study of the first excited levels of Ar

In the MSE-sustained plasma the excited atoms are produced between the electrodes as well as above the cathode by electron impact excitation, dissociative recombination, radiative cascading from higher excited levels, ion and fast neutral collisions and photo excitation [19].

The first four excited states of Ar are two metastable and two resonance levels (figure 2). The metastable levels are $1s_5$ and $1s_3$ (Paschen notation) at 11.55 and 11.72 eV above the $1p_0$ ground state, respectively. The lifetime of the metastable levels is 55.9 s for the $1s_5$ and 44.9 s for $1s_3$ [20]. The resonance levels lie close to the metastable levels, i.e. the $1s_4$ level at 11.62 eV and the $1s_2$ level at 11.83 eV. The lifetime of the resonance levels is 9.5 ns and 0.24 ns for $1s_4$ and $1s_2$, respectively [21]. The metastable levels have forbidden dipole transition to the ground state, which determines their long lifetime. The resonance levels can decay to the ground state by radiation emission at 106.666 nm ($1s_4$–$1p_0$) and 104.822 nm

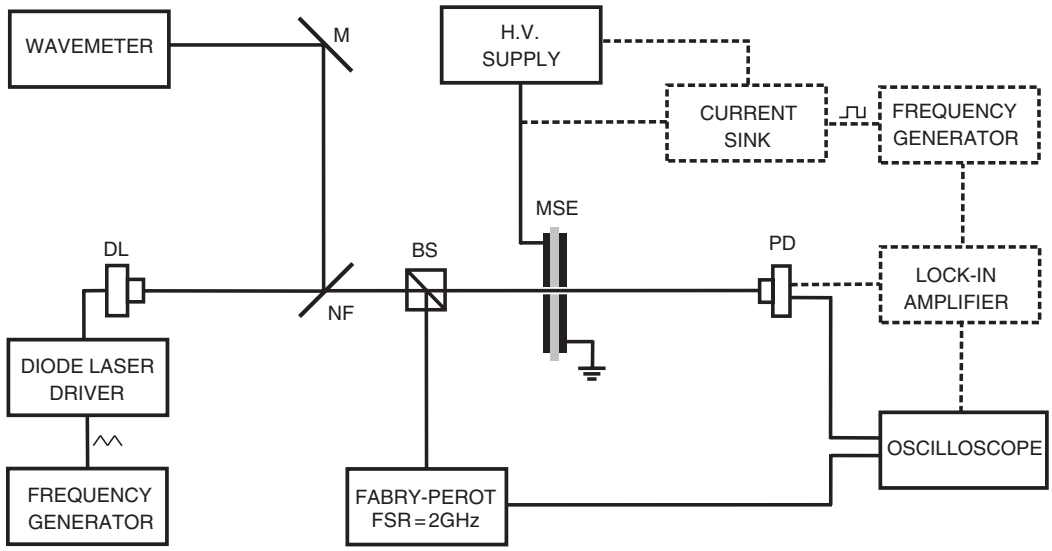

Figure 3. Experimental set-up for DL absorption measurements through the MSE discharge channel.

($1s_2$–$1p_0$). In practice, these resonance states are also long-lived due to resonance radiation trapping and collision transfer processes with the near-lying metastable states. In high-pressure discharges these effects result in a lifetime of the resonance levels comparable with that of the metastable levels.

The density N_i ($i = 2$–5) of the $1s_i$ level can be calculated using the relation [22]:

$$\int k_\nu \, \mathrm{d}\nu = \lambda_{0i}^2 \frac{g_j}{g_i} \frac{A_{ji}}{8\pi} N_i \left(1 - \frac{g_j}{g_i} \frac{N_j}{N_i}\right) \tag{1}$$

For the i–j transition λ_{0i} is the central wavelength, g_i and g_j are the statistical weights of the lower and upper level and A_{ji} the spontaneous emission probability.

The absorption coefficient k_ν is derived from the Beer–Lambert law as:

$$k_\nu l = \ln\left(\frac{I_0}{I_\nu}\right) \tag{2}$$

where I_0 is the intensity of the transmitted radiation in the absence of absorbers, I_ν the transmitted intensity at the frequency ν in the presence of absorbers and l the absorption length. The term $\ln(I_0/I_\nu)$ is known as the optical depth.

In noble gas discharge plasmas the density of the upper level N_j is at least three orders of magnitude smaller than that of the N_i level, if 1s–2p transitions are considered. Therefore, the density N_i of the lower level is given by

$$N_i = \frac{\int k_\nu \, \mathrm{d}\nu}{\lambda_{0i}^2 (g_j/g_i)(A_{ji}/8\pi)} \tag{3}$$

The quantities $\lambda_{0i}^2 (g_j/g_i)(A_{ji}/8\pi)$ are given in table 2 for the studied transitions.

Passing the DL beam through the MSE hole, the transmitted laser intensity was measured and the absolute number density of the excited atoms was calculated using equation (3). The evaluation of the absolute number density of the excited levels is rather difficult because the absorption length cannot be precisely determined in our case and due to the fact that the plasma is not completely homogeneous. As can be seen from figure 1, the excited atoms are not uniformly distributed in the discharge. Furthermore the optical appearance of the microdischarge changes with pressure, i.e. at 50 mbar on the discharge axis the light emission shows a maximum, while at 400 mbar it shows a minimum. As absorption occurs inside the MSE hole and above the cathode as well, a minimum and a maximum absorption length were considered.

Table 2. Transitions studied in the present work and their characteristics.

λ_0 (nm)	E_i (eV)	E_j (eV)	g_i	g_j	A_{ji} (s^{-1})	$\lambda_{0i}^2(g_j/g_i)\times(A_{ji}/8\pi)$ ($m^2\,s^{-1}$)
801.699	11.549	13.095	5	5	9.553×10^6	2.40×10^{-7}
800.838	11.624	13.172	3	5	4.657×10^6	1.98×10^{-7}
772.633	11.723	13.328	1	3	1.271×10^7	9.05×10^{-7}
826.680	11.828	13.328	3	3	1.680×10^7	4.57×10^{-7}

For calculating the absolute number density, the maximum value for the total absorption length was taken as the sum of the length of the hole and the plasma length outside the hole. The plasma length outside the hole was evaluated from spatially resolved absorption measurements above the cathode as the distance from the cathode surface to the point where the absorption signal decreases to approximately 10% from its maximum value. The minimum absorption length was taken as the sum between a third of the hole length and the distance from the cathode to the point where the light intensity diminishes to 20% from its maximum value. As an example, at 50 mbar the maximum and the minimum absorption length considered were 1100 μm and 600 μm, respectively. At 400 mbar the maximum lies at 300 μm and the minimum at 50 μm. Furthermore, when only an effective absorption area is considered the absolute number density increases by a factor of two. Under these conditions, the errors in determining the absolute number density are in the range of about $\pm$50%.

Figure 4 presents the variation of the absolute number density with pressure for the first four excited levels of Ar. For

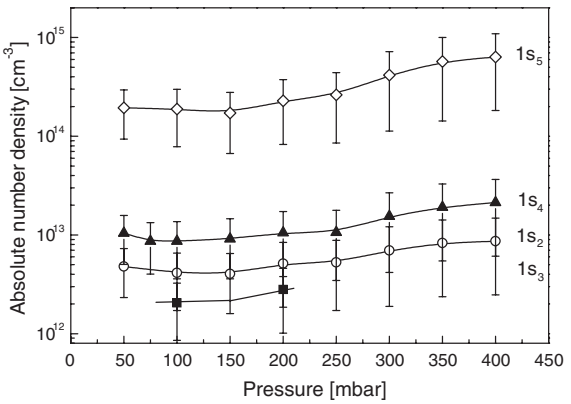

Figure 4. Absolute number density of the $1s_i$ ($i = 2$–5) excited levels of Ar in the MSE-sustained discharge for the pressure range 50–400 mbar.

the metastable $1s_3$ level only two values were obtained because the DL used for probing this transition was destroyed during the measurements. In the pressure range 50–400 mbar the absolute number density values vary from 1.9×10^{14} to 6.3×10^{14} cm^{-3} for the lowest $1s_5$ level and from 4.8×10^{12} to 8.8×10^{12} cm^{-3} for the highest $1s_2$ level. Within this relatively high uncertainty it can be seen that the density slightly increases with pressure mostly due to the rise in the current density.

It should be stressed that inside the hole of the MSE both the production and the destruction of excited states are very efficient. Due to the high current density a large number of excited atoms are produced, especially in the negative glow adjacent to the cathode. Since the geometrical dimensions of the hole are small, diffusion becomes important in the destruction of the excited species in spite of the high pressure. The excited atoms easily reach the walls of the hole where they are strongly quenched. Other processes that are responsible for the depopulation of the excited levels are the two- and three-body collisions, whose importance rises with pressure. In the region outside the hole the density of charged particles is lower than inside the hole and it is expected that only a small fraction of excited atoms are produced by electron impact. The plasma volume above the cathode surface can be considered a spatial afterglow, where the excited atoms are mostly created in recombination processes and by photo-excitation or absorption of the resonance radiation escaping from the hole. The destruction mechanisms above the cathode are partially different: the depopulation of the excited levels occurs mostly due to volume processes like two- and three-body collisions, quenching due to impurities. Indeed, measuring without gas flow through the chamber it was observed that the density of excited atoms strongly decreases with time.

5. Gas temperature and electron density

5.1. Theoretical considerations

In discharge plasmas different mechanisms contribute to the broadening of the atomic transition lines. In high-pressure plasmas the line profiles are mainly broadened and shifted due to the thermal movement of the atoms, their frequent collisions with neutrals and their interaction with charged particles.

If the absorbing atoms have a Maxwell velocity distribution characterized by a temperature T, the intensity profile of a Doppler broadened spectral line follows a Gauss distribution. The FWHM $\Delta\lambda_G$ of this distribution is related to the temperature T by [23]:

$$\Delta\lambda_G = 7.16 \times 10^{-7}\lambda_0\sqrt{\frac{T}{M}} \tag{4}$$

where M is the atomic mass of the absorbing particle and λ_0 the central wavelength of the transition.

Pressure broadening is a consequence of the interaction between the excited atoms under consideration and neutral particles (collision broadening) and of the micro-fields created by charged particles (Stark broadening). The interaction of the absorbing atoms with neighbouring neutral atoms generates a broadening of the line profile and also a shift of its central wavelength. The relations that give FWHM and the shift for the collision broadening are

$$\Delta\lambda^{\text{coll}}_{\text{Lwidth}} = 2\gamma N \tag{5}$$

$$\Delta\lambda^{\text{coll}}_{\text{Lshift}} = \beta N \tag{6}$$

where N is the neutral particle density and 2γ and β are the collision broadening parameters specific for each transition.

Stark broadening is caused by the Coulomb interaction of the absorbing atom with the charged particles present in the plasma. The non-hydrogenic atoms are subject to quadratic Stark effect, which induces a broadening and a shift of the line. In this case, the FWHM $\Delta\lambda^{\text{Stark}}_{\text{Lwidth}}$ and the shift $\Delta\lambda^{\text{Stark}}_{\text{Lshift}}$ are complex functions of the electron density N_e and electron temperature T_e. The expressions for the Stark broadening and shift can be approximated by [24]

$$\Delta\lambda^{\text{Stark}}_{\text{Lwidth}} = 2 \times \left[1 + 1.75 \times 10^{-4} N_e^{1/4}\alpha \times \left(1 - 0.068 N_e^{1/6} T_e^{-1/2}\right)\right] \times 10^{-16} w N_e \tag{7}$$

$$\Delta\lambda^{\text{Stark}}_{\text{Lshift}} = \left[\frac{d}{w} + 2 \times 10^{-4} N_e^{1/4}\alpha \left(1 - 0.068 N_e^{1/6} T_e^{-1/2}\right)\right] \times 10^{-16} w N_e \tag{8}$$

where w is the electron impact width, d/w is the relative shift and α is the ion broadening parameter, all given in [25].

Collision and Stark broadened line profiles have a Lorentzian intensity distribution. The total Lorentz contribution $\Delta\lambda^{\text{total}}_{\text{Lwidth}}$, assuming there is no correlation between the two effects, is given by

$$\Delta\lambda^{\text{total}}_{\text{Lwidth}} = \Delta\lambda^{\text{coll}}_{\text{Lwidth}} + \Delta\lambda^{\text{Stark}}_{\text{Lwidth}} \tag{9}$$

A similar relation holds for the shift of the line. The convolution of the Gauss and Lorentz distributions is the Voigt profile. The approximate equation relating the Voigt, Gauss and Lorentz FWHM is given in [26]

$$\Delta\lambda_G^2 = \Delta\lambda_V^2 - \Delta\lambda_V \cdot \Delta\lambda^{\text{total}}_{\text{Lwidth}} \tag{10}$$

The main idea here is to separate the Gauss contribution (which dominates the profile near the line centre) and the Lorentz contribution (which governs the wings of the line).

The procedure was the following: first the total Voigt width and shift $\Delta\lambda_V$ were determined from the experimentally recorded optical depth $\ln(I_0/I_\nu)$. For the evaluation of the total Lorentz contribution, the values of the optical depth were measured far out in the wings of the absorption line where the Lorentz distribution $P(\lambda)$ can be approximated by

$$P(\lambda) = \frac{A}{2\pi} \frac{\Delta\lambda_{\text{Lwidth}}^{\text{total}}}{(\lambda - \lambda_0)^2} \tag{11}$$

where A is the integral of the measured absorption profile and $(\lambda - \lambda_0)$ is the distance from the line centre. The Gauss width was calculated using equation (10). Further, the collision contribution calculated with the broadening parameters given in [27] and [28] was extracted from the total Lorentz width and the remaining part was ascribed to Stark broadening.

5.2. Plasma parameters and discussion

The line profiles of the 801.699 nm Ar transition at two different pressures, 50 and 400 mbar are presented in figure 5. It can be seen that the line width and the shift of the central wavelength are strongly increasing with the pressure. For the evaluation of the plasma parameters only the transitions at 801.699 and 800.838 nm were studied. The main reason for the restriction of the analysis to these lines is their large optical depth. The analysis of the transition at 772.633 nm could not be pursued, since the collision broadening parameters were not found in the literature. The line at 826.680 nm is too broad (FWHM more than 10 pm at 400 mbar) for a mode-hope free laser diode tuning over the line and the far wings.

5.2.1. Gas temperature. According to the model previously presented, the absorption line profiles of the $1s_5$–$2p_8$ Ar transition at 801.699 nm were deconvoluted and the Gauss contribution to the line profile was extracted. Using equation (4), the temperature was calculated and the results are presented in figure 6 for the pressure range 50–400 mbar. In the same figure the temperature obtained from the analysis of the line profile of the $1s_4$–$2p_6$ transition at 800.838 nm is also shown. It can be seen that there is a good agreement between the data obtained from the two transitions, which gives confidence in the accuracy of the results.

The gas temperature increases with pressure. By increasing the pressure the electron mean free path reduces, the electrons gain less energy between collisions and transfer more energy to the gas. As the power input in the discharge is constant and the plasma volume decreases with pressure, it results in a higher current density and consequently to a more pronounced heating of the gas. Note that the gas temperature corresponds to the plasma region with the highest population density. Thus, for pressures higher than about 200 mbar these measurements give the gas temperature of the discharge confined inside the hole of the MSE.

5.2.2. Evaluation of the electron number density. The total Lorentz contribution was measured experimentally far in the wings of the absorption line profiles for the transitions at 801.699 and 800.838 nm. Figure 7(*a*) shows the results for the transition from the metastable $1s_5$ level and the collision broadening contribution, taking into account equations (5) and (6) and the data given in table 3. For the 801.699 nm line the values of the broadening coefficients from table 3 were adjusted to the discharge temperature using the $T^{0.3}$ dependence (Lindholm–Foley theory). The broadening parameters for the 800.838 nm transition, which connects the resonance $1s_4$ level with the $2p_6$ state, were assumed to be temperature-independent. The neutral gas density was determined using the ideal gas law considering the discharge pressure and the temperature previously estimated. For both transitions investigated, a big difference between the total Lorentz width and the collision broadening width was observed. This difference is ascribed to the quadratic Stark effect and can be described by equation (7).

As predicted by the theory, the central wavelength of the transition from the metastable $1s_5$ level is shifted. This shift increases with pressure (see figure 5). The experimentally measured and theoretically calculated collision shift are plotted for comparison in figure 7(*b*). In the case of the transition from the resonance $1s_4$ level, the line shift is very small (less than 1 pm at 50 mbar) and is pressure-independent. The errors in evaluating the experimental shift are rather large due to the fact

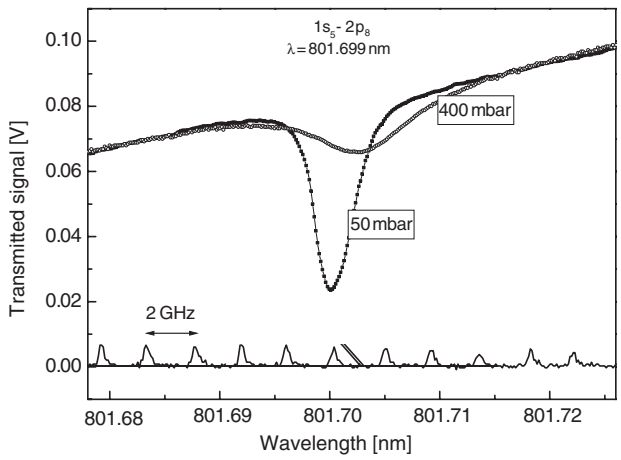

Figure 5. Effect of the pressure in the absorption line shape for the 801.699 nm line.

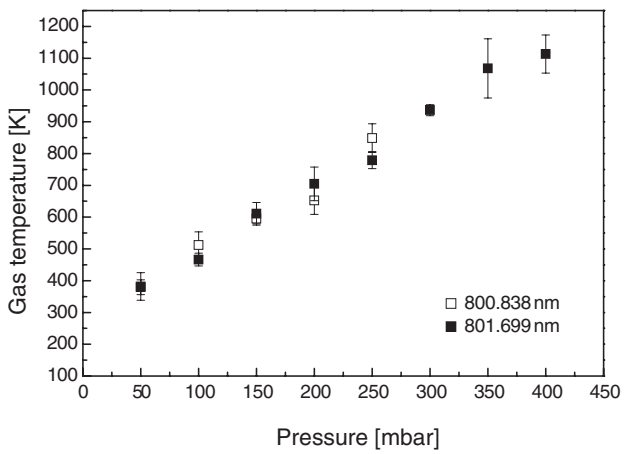

Figure 6. Gas temperature in the microdischarge derived from the $1s_5$–$2p_8$ and $1s_4$–$2p_6$ transitions.

that it was not possible to measure the central wavelength very precisely (wavemeter accuracy 1 pm).

Subtracting the collision contribution from the total Lorentz width and shift, the electron density was estimated from equations (7) and (8), using the Stark broadening parameters listed in table 4. The electron temperature was assumed to be about 1 eV taking into account the results presented in [29]. A small variation of this value has no significant influence on the calculated electron density. The electron number density cannot be given very accurately because different values of the collision width and shift could be found in the literature (see figure 7 and table 3). The range of electron density is presented in figure 8, where the values of the collision broadening parameters were taken from different publications. It can be seen that the electron number density increases by a factor of 5 in the pressure range 50–400 mbar. The present measurements give the electron number density in the discharge area, i.e. inside the MSE hole. Taking into account the density of neutral atoms and the electron density it can be concluded that the degree of ionization in the MSE-sustained discharge is about 10^{-3}.

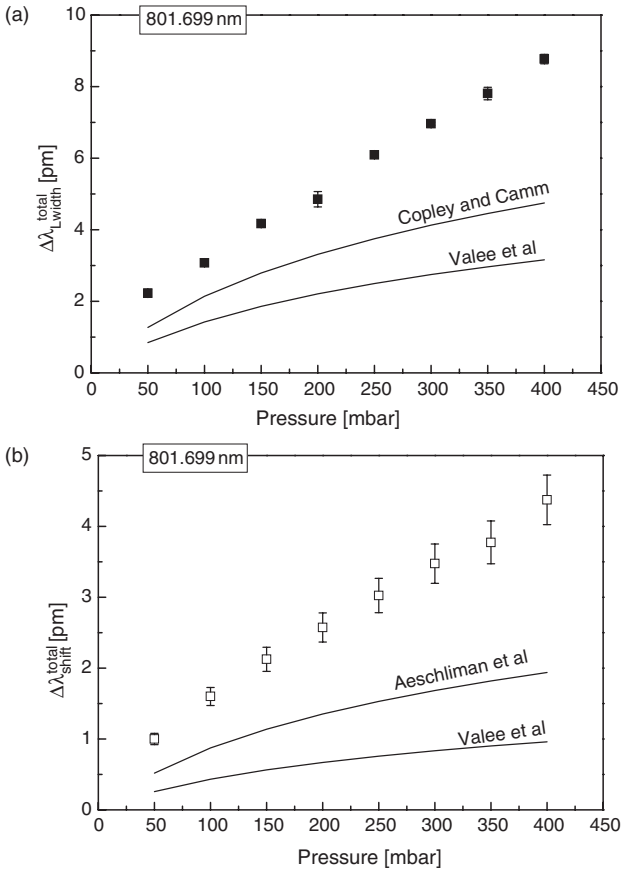

Figure 7. Measured width (*a*) and shift (*b*) due to pressure broadening for the transition at 801.699 nm (■) and calculated values (——).

6. Conclusions

In this work, the absolute population density of the excited $1s_5$, $1s_4$, $1s_3$, and $1s_2$ levels of Ar was measured and the gas temperature and the electron number density were calculated from the absorption line profiles taking into account significant broadening mechanisms.

To our knowledge, absorption spectroscopy of the excited atoms in high-pressure dc glow discharges was reported up to now only in [30]. The authors measured the population density of the $6s[3/2]_2$ level of Xe for pressures lower than 100 mbar in a hollow cathode discharge with 2 mm electrode gap. The results concerning the number density of excited atoms presented in this work are comparable with the absolute metastable Xe $6s[3/2]_2$ density reported in [30].

The gas temperature in a high-pressure small-size discharge operated in nitrogen [29] may reach values of about 1000 K at 200 mbar. Taking into account that the input power for a discharge operating in nitrogen is significantly higher than in Ar, the gas temperature obtained in our measurements is realistic. Although the plasma confined inside the hole may reach gas temperatures up to 1000 K, the ambient gas temperature immediately above the microstructure exceeds only slightly the room temperature.

The electron number density measured in the present work is comparable with data reported in [29], where the Stark broadening of the Balmer H_β line was measured by emission spectroscopy in a mixture of Ar + 20% H_2 on a similar discharge geometry.

Since the experimental diagnostics of high-pressure plasmas is not always easy to perform, results concerning the plasma parameters are often extracted from modelling. For comparison, in the case of plasma display panels [31] the electron number density and the density of excited atoms were found to be at least one order of magnitude lower than in the case of the studied MSE discharge, while the gas temperature is close to room temperature. Regarding other high-pressure discharges, like glow discharges or classical dielectric barrier discharges at atmospheric pressure only few results are available [4, 10].

It can be concluded that the study of the MSE-sustained high-pressure discharge by DL absorption spectroscopy revealed valuable information about the excited species and about plasma parameters. Due to the high number density of excited atoms in metastable and resonance states produced

Table 3. Line broadening and line shift coefficients for Ar lines from [27]. The gas temperature of the plasma source is indicated in brackets.

Transition (nm)	$2\gamma/N$ (10^{-20} cm^{-1} cm^3)	β/N (10^{-20} cm^{-1} cm^3)	Authors
801.699	2.8 ± 0.3 (3900 K)	8.5 ± 0.5 (3900 K)	Vallee *et al*
	2.9 ± 0.3 (1130 K)	15.1 (1130 K)	Copley and Camm
		7.95 ± 0.39 (300 K)	Aeschliman *et al*
800.838	3.54 ± 0.39 (300 K)	3.7 ± 0.19 (300 K)	Aeschliman *et al*
	4.05 ± 0.2 (1130 K)		Copley and Camm

Table 4. Stark broadening parameters [25] for the Ar transitions 801.699 and 800.838 nm for an electron temperature of about 1 eV.

Transition (nm)	Stark parameters	5000 K	10 000 K	20 000 K
801.699	w	0.037	0.049	0.065
	d/w	1.630	1.340	0.990
	α	0.038	0.031	0.025
800.838	w	0.036	0.047	0.062
	d/w	1.650	1.380	1.030
	α	0.040	0.032	0.026

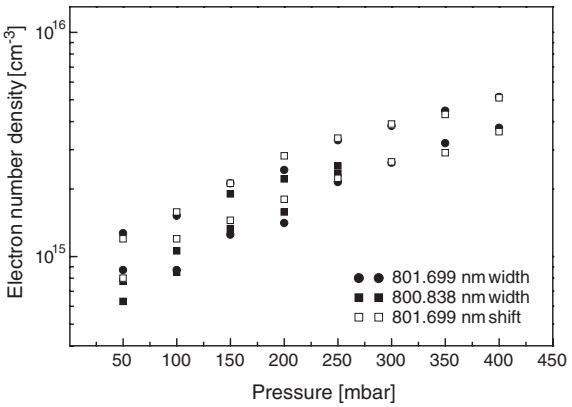

Figure 8. Electron number density in the MSE-sustained discharge as a function of pressure at constant current.

in the microdischarge, the DLAAS technique has been successfully applied in spite of the very short absorption length (hundreds of μm) provided by the MSE plasma. It should be mentioned that this technique is an innovative approach for investigating sub-millimetric discharges.

Acknowledgments

The authors would like to thank Dr J Franzke and Dipl. Phys. K Kunze (ISAS Dortmund, Germany), Professor Dr K Wiesemann (Bochum University, Germany) and Dr N K Bibinov, (Research Institute of Physics, St Petersburg, Russia) for fruitful discussions. Special thanks are addressed to the Company Atomika Instruments GmbH for the financial support of Dr M Miclea. Financial support from Bundesministerium für Bildung und Forschung (BMBF), Verein Deutsche Ingenieure (VDI) and Graduiertenförderung Land Hessen is also gratefully acknowledged.

References

[1] Goldman M and Goldman T 1978 Corona discharges *Gaseous Electronics 1, Electrical Discharges* (New York: Academic)
[2] Okazaki S, Kogoma M, Uehara M and Kimura Y 1993 *J. Phys. D: Appl. Phys.* **26** 889–92
[3] Kogelschatz U, Elliason B and Egli W 1997 *Proc. XXIIIrd ICPIG (Toulouse)* pp C4–47
[4] Frame J W and Eden J G 1998 *Electr. Lett.* **34** 1529
[5] Shi W, Stark R H and Schoenbach K H 1999 *IEEE Trans. Plasma Sci.* **27** 16–17
[6] Mildner M, Korzec D and Engemann J 1999 *Surf. Coat. Technol.* **112** 366–72
[7] Bilgic A M, Engel U, Voges E, Kückelheim M and Brockaert J A C 2000 *Plasma Sources Sci. Technol.* **9** 1–4
[8] Bräuning-Demian A, Spielberger L, Penache C and Schmidt-Böcking H 2000 *Proc. XIII Int. Conf. on Gas Discharges and their Applications (Glasgow)* pp 426–9
[9] Penache C, Bräuning-Demian A, Spielberger L and Schmidt-Böcking H 2000 *Proc. Hakone VII (Greifswald)* vol 2, pp 501–5
[10] Massines F, Rabehi A, Decomps P, Gadri R B, Segur P and Mayoux C 1998 *J. Appl. Phys.* **83** 2950–7
[11] Kurunczi P, Shah H and Becker K 1999 *J. Appl. Phys. B: At. Mol. Opt. Phys.* **32** 656–8
[12] Moselhy M, Stark R H, Schoenbach K H and Kogelschatz U 2001 *Appl. Phys. Lett.* **78** 880–2
[13] El-Habachi A, Shi W, Moselhy M, Stark R H and Schoenbach K H 2000 *J. Appl. Phys.* **88** 3220–4
[14] Kogelschatz U, Eliasson B and Esrom H 1991 *Mater. Design* **12** 251–8
[15] Franzke J, Schnell A and Niemax K 1993 *Spectrochim. Acta Rev.* **15** 379–95
[16] Kunze K, Miclea M, Musa G, Franzke J, Vadla C and Niemax K 2002 *Spectrochim. Acta* (part B) **57** 137–46
[17] Penache C, Gessner C, Bräuning-Demian A, Scheffler P, Spielberger L, Hohn O, Schössler S, Jahnke T, Gericke K-H and Schmidt-Böcking H 2002 Spectroscopy of non-equilibrium plasma at elevated pressures *Proc. SPIE* **4460** 17–25
[18] Zybin A, Schnürer-Patschan C and Niemax K 1995 *J. Anal. At. Spectrom.* **10** 563–7
[19] Gordon F 1956 *Encyclopedia of Physics, vol XXII—Gas Discharges II* (Berlin: Springer)
[20] Filipovic D M, Marinkovic B P, Pejcev V and Vuskovic L 2000 *J. Phys. D: At. Mol. Opt. Phys.* **33** 2081–94
[21] Smith P L, Heise C, Esmond J R and Kurucz R L *Atomic Spectral Line Database* from CD-Rom 23 of R L Kurucz http://cfa-www.harvard.edu/amdata/ampdata/kurucz23/sekur.html.
[22] Mitchell A and Zemansky M 1971 *Resonance Radiation and Excited Atoms* (Cambridge: Cambridge University Press) pp 95–6
[23] Demtröder W 1996 *Laser Spectroscopy* (Berlin: Springer)
[24] Huddlestone R and Leonard S 1965 *Plasma Diagnostic Techniques* (New York: Academic) p 277
[25] Griem H 1962 *Phys. Rev.* **128** 515–21
[26] Whiting E E 1968 *J. Quant. Spectrosc. Radiat. Transfer* **8** 1379–84
[27] Moussounda P S and Ranson P 1987 *J. Phys. B: At. Mol. Phys.* **20** 946–61
[28] Tachibana K, Harima H and Urano Y 1982 *J. Phys. B: At. Mol. Phys.* **15** 3169–78
[29] Petzenhauser I, Ernst U, Hartmann W and Frank K 2001 *Proc. APP Spring Meeting 'Diagnostics of Non-Equilibrium High-Pressure Plasmas' (Bad Honnef)* pp 217–20
[30] Bussiahn R and Lange H 2001 *Proc. APP Spring Meeting 'Diagnostics of Non-Equilibrium High-Pressure Plasmas' (Bad Honnef)* pp 175–8
[31] Meunier J, Belenguer Ph and Boeuf J P 1995 *J. Appl. Phys.* **78** 731–45